

## Strength of R/C shell panel under combined loadings

\* Takashi Hara <sup>1)</sup>

<sup>1)</sup>Department of Civil Engineering and Architecture, Tokuyama College of Technology,  
Shunan, Japan

<sup>1)</sup> [t-hara@tokuyama.ac.jp](mailto:t-hara@tokuyama.ac.jp)

### ABSTRACT

In this paper, the load bearing capacity and the deformation characteristics of Reinforced Concrete (R/C) cylindrical shell panel were investigated experimentally and numerically under combined axial and flexural loading conditions. R/C shell has 980 x 980mm plan and 10mm thickness. The radius of the shell is 689mm. It consists of micro-concrete and steel mesh of 0.75mm diameter with 5mm openings. R/C shell is pin supported at all edges. In this analysis, the concentrate load was applied combined with axial compressive force. In numerical analysis, the ultimate strength of R/C shell was investigated in the same conditions as experiments. In experimental analysis, R/C shell panels were tested under the same loading and boundary conditions. Comparing both results, the ultimate strength of R/C shell panels was discussed.

### 1. INTRODUCTION

R/C shell structures have been applied to the industrial and social facilities due to their high load bearing capacities and the lightness of the structure. These structures are subjected to several loadings. Therefore, they should be designed under the combined loading conditions. In this paper, the load bearing capacity and the deformation characteristics of R/C cylindrical shell panel were investigated experimentally and numerically under combined axial and flexural loading conditions. R/C shell panel has 980 x 980mm plan and 10mm thickness. The radius of the shell panel is 689mm. It consists of micro-concrete and steel mesh of 0.75mm diameter with 5mm openings. R/C shell panel is pin supported at all edges. In numerical analysis, the concentrate load was applied combined with axial compressive force. R/C shell panel was modeled by degenerated finite elements and nonlinear analysis was performed using material test data. In the loading tests, two types of compressive loading conditions are applied. One was the R/C shell panel under axial compression. The other was the R/C panel without axial compression. After applying the axial load, the lateral load was applied gradually. From the experimental analyses, the conditions of combined stresses on R/C shell surface improved the flexural rigidities of the shell

---

<sup>1)</sup> Professor

panel and also improved the strength of the shell panel as well. Then, numerical results were compared with experimental data and were well simulate the experimental results.

**2. EXPERIMENTAL MODEL**

Fig. 1 shows the geometric configuration of R/C shell panel adopted in this analysis. The thickness of the shell is 10mm. The radius of it is 689mm and the ratio of the rise and the span is 1/5. The plan of the panel is 950mm and 960mm in hoop and meridional directions, respectively. The micro concrete was used to make R/C shell panel. The weight ratio of the water to the cement and the sand is two and four, respectively. R/C shell panel contains the wired mesh of  $\phi$  0.75mm diameter and 5mm spacing in both hoop and meridional directions. The mesh was placed in the middle of R/C shell panel. The material data was obtained from the material tests. The material data of the micro concrete and the wired mesh is shown in Table 1.

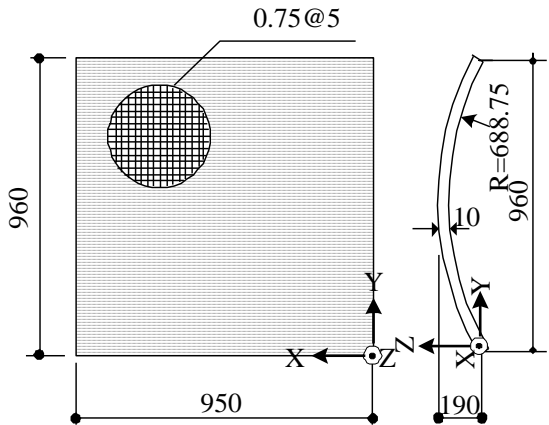


Fig.1 R/C cylindrical panel

Table 1 Material properties

Concrete		Reinforcement	
Compressive Strength	38.1	Yield Stress(MPa)	235
Tensile Strength(MPa)	3.6	Tensile Stress(MPa)	449
Young's Modulus(GPa)	22.3	Young's	206
Poisson's Ratio	0.20		

**3. EXPERIMENTAL MODEL**

*2.1 Experimental Setup*

Fig.2 shows the experimental apparatus adopted in this paper. R/C shell panel is pin supported on meridional edges along the guide rails which are fixed on the supporting frame. The detail of the support on the meridional edge is shown in Fig. 3. The supports consist of a steel ball in the socket and can rotate freely. Also, one end of the hoop edge is pin supported on the reaction wall as shown in Fig. 4. Each pin has the same function as that of the meridional edge. The hoop edge of R/C shell is

supported by pins on both upper and lower side of the panel. The other side is pin supported as the same manner but can translate into axial direction.

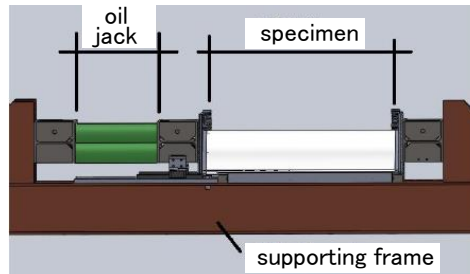


Fig.2 Experimental apparatus



Fig.3 Meridional pin supports



Fig.4 Hoop pin supports

### 2.2 Experimental results

In experiment, two types of specimens are adopted. One is the specimen without axial compression (SP0). The other is the specimen with axial compressive force 40kN (SP4). After compressive loading was loaded via axial oil jack and the compressive load was held during experiment. Then, concentrate lateral loading was applied gradually at the center of the panel plane for each specimen. In experiment, strains in both hoop and meridional directions and the lateral deflections were measured at equidistance points on the panel surface.

Load deformation properties Fig. 6 and Fig. 7 show the load deformation relation of the specimen SP0 (without axial compression) and SP4 (axial compression 40kN), respectively. The numbers represented in the figure denotes the loading points shown (see intermediate figure). Comparing these figures, the stiffness of the panel under compressive load shows greater ratio than that without axial compressive force. The ultimate strength of R/C panel under compressive force is larger than that without axial compressive force. However, the difference between them shows small.

Crack patterns Fig. 8 and Fig. 9 show the crack pattern of the R/C panel after peak loading. Fig.8 shows the cracks only under lateral load. Cracks spread within wide range of panel surfaces. Fig. 9 also shows the crack patterns under combined axial compressive and lateral loadings. The cracks are concentrated into the loading portion.

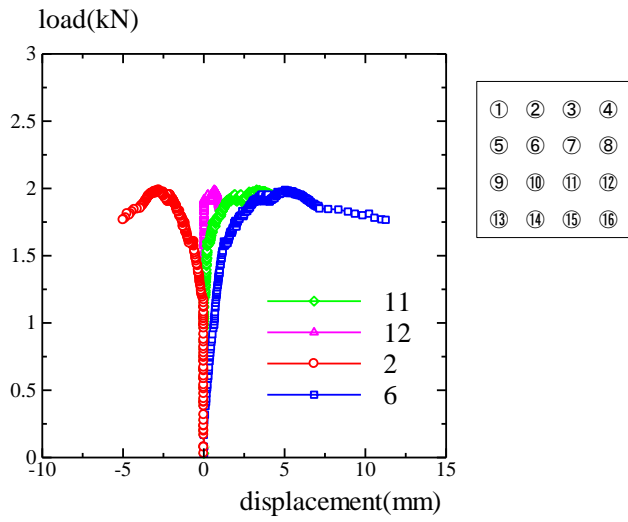


Fig. 6 Load deformation relation (SP0)

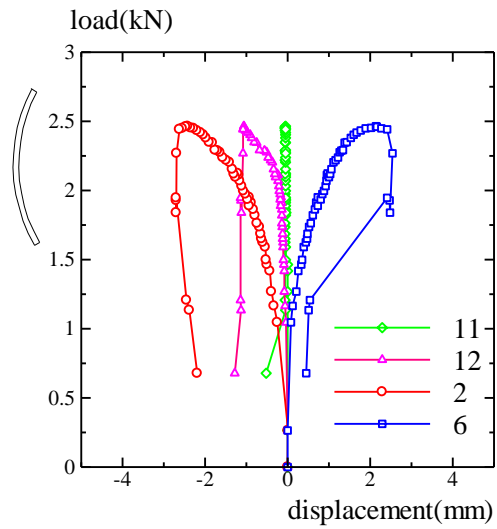
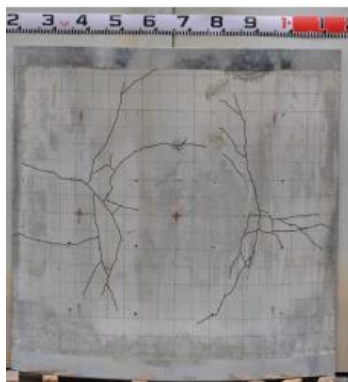
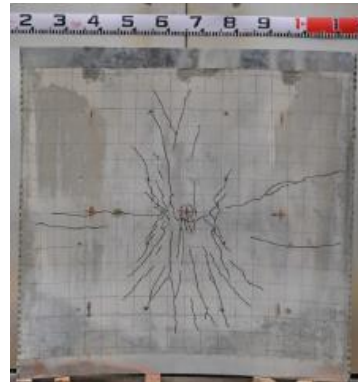


Fig. 7 Load deformation relation (SP4)



Outer surface



Inner surface

Fig. 8 Crack pattern of R/C panel without axial compression (SP0)



Outer surface



Inner surface

Fig. 9 Crack pattern of R/C panel with axial compression (SP4)

## 4. NUMERICAL ANALYSIS

In numerical analyses, the finite element procedure is applied. Fig. 10 shows the FE mesh of R/C panel. The panel is divided into 32 elements in both meridional and hoop directions, respectively. Shell elements are divided into 8 concrete layers and 2 steel layers based on the layered approach (Hara 2011 and Hinton 1984). Boundary conditions are pin supported at all edges.

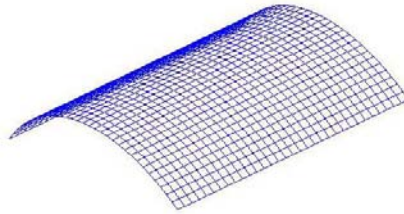
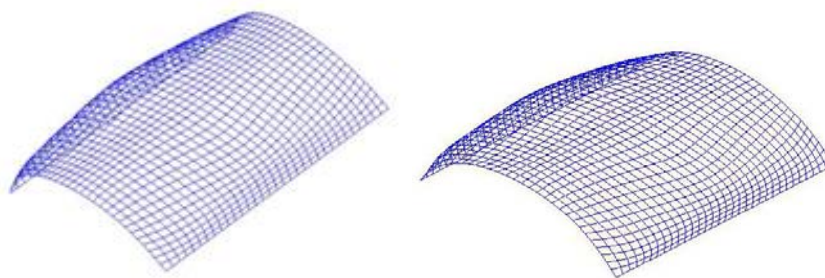


Fig.10 FE mesh

### 4.1 EM procedure and numerical assumptions

In numerical analysis, the degenerate shell element is adopted and the geometric and material nonlinearities are taken into account. 9 nodes Heterosis element is used and  $2 \times 2$  reduced integration is performed to avoid the numerical problems. The numerical simulation is performed under the displacement incremental scheme. The yield condition of concrete is defined as the Drucker-Prager type, which is assumed that concrete yields when the equivalent stress based on mean stress and second deviatoric stress invariants reaches uniaxial compressive strength (Hinton 1984). The crushing condition is controlled by strains. The ultimate compressive strain of concrete is assumed as 0.003 by Kupfer's experiment (Kupfer 1969). Also, after cracking of concrete, the tension stiffening parameters accounting for the tensile strength of concrete are introduced. The material nonlinearities of steel are assumed to be bilinear stress-strain relation for the reinforcement.



SP0

SP4

Fig. 11 Deformation pattern of R/C panel

### 4.2 Numerical results

Fig. 11 shows the deformation of R/C shell panel subjected to a concentrate load at the panel center. R/C shell is pin supported at all edges. SP0 and SP4 are subjected to 0kN and 40kN axial compressive force, respectively. The deformation properties and

the crack distribution is the same as experimental results. Fig. 12 shows the relation between axial compressive force and the ultimate strength of lateral concentrate loadings.

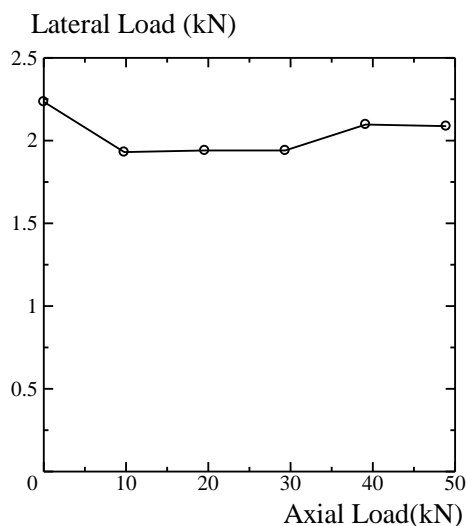


Fig.12 Relation between axial compression and lateral loading

## 5. CONCLUSIONS

In this paper, the numerical and experimental analyses of the R/C cylindrical shell panel were performed under combining the axial compressive and lateral force. From both numerical and experimental analyses, following conclusions are obtained.

- (1) The axial compressive force improved the stiffness of the R/C shell panel subjected to the lateral load. R/C shell panel subjected to axial compressive force shows small deformation.
- (2) The cracks concentrate at the loading point under both compressive axial and lateral loads but the cracks spread widely on R/C shell panel when the axial load is not applied.
- (3) The ultimate strength of R/C shell panel is not strongly dependent on the axial compression.
- (4) Numerical results well simulate the experimental behavior of R/C shell panel.

## REFERENCES

- Hara, T. (2011). "Application of computational technologies to R/C structural analysis", *Computers & Concrete*, **8**(1), 97-110
- Hinton, E., and Owen, D.J.R. (1984). "*Finite element software for plates and shells*", Prineridge Press, Swansea.
- Kupfer, H., and Hilsdorf, K.H. (1969). "Behaviour of concrete under biaxial stress", *ACI Journal* **66**(8), 656-666.